Parametric Investigations on Industrial Size Heat Pipe

Pranav Oza[1], Aum Chavda[2], S V Jain[3], Anand Bhatt[4]
[1,2,3,4] *Mechanical Engineering Department, School of Engineering, Institute of Technology, Nirma University, Ahemdabad-382481, Gujarat, India*

***Abstract*—A heat pipe is a device that transfers heat from a source of high temperature to a sink of low temperature. It's a kind of heat exchanger that uses phase transition to transmit heat. The pressure inside the heat pipe, the number of wick layers, the filling ratio, the hdeat input, the orientation of the heat pipe, and the mass flow rate of water are some of the variables that affect how well a heat pipe performs. The current study's objective is to perform a parametric analysis of heat pipes with different filling ratios (20%, 30%, 40%, and 50%), heat input within the pipes (400W to 1500W) with one wick layer while maintaining constant atmospheric pressure, 45° heat pipe orientation, and 2.66 ml/sec water mass flow rate. The results of the calculations are displayed in terms of temperature profile of the heat pipe, effectiveness, overall heat transfer coefficient, evaporation heat transfer coefficient, condensation heat transfer coefficient, overall thermal resistance, evaporation heat transfer coefficient, and temperature vs. heat input of the heat pipe. The parametric experiments revealed that at a 40% filling ratio and 600 W, the maximum heat pipe efficiency was 88.53%.**

***Abstract*—Filling ratio, Heat pipe, Pressure, Wick, Optimization**

1. INTRODUCTION

Heat Pipe is a closed loop system in which heat transfer takes place. Heat pipes work by including evaporation, condensation, and adiabatic phenomena altogether. Heat pipe contains a fluid inside it which is known as working fluid. Working fluid in a Heat Pipe Heat Exchanger (HPHE) system absorbs heat from an external heat source at the evaporator section and transforms into a gaseous phase. This gaseous working fluid then travels via an adiabatic section to the condenser section because of a pressure differential. The condenser transfers heat to the cold fluid on the other end. It was noted that the evaporator and condenser sections of the heat pipe might see an increase in the heat transfer coefficient to more than 1500 W/m^{2}K [1]. The reason behind this is the phase change of the working fluid inside the heat pipe. Heat Exchangers (HPHEs) provide numerous advantages over conventional heat exchangers, including the ability to operate at small temperature differences, minimal pressure variation in the external fluid flow, a significant increase in thermal conductivity and heat flux, and advantages during manufacturing [2]. A heat pipe consists of three main sections: the evaporator, the adiabatic section, and the condenser. In the evaporator section, heat is absorbed by the working fluid, causing it to vaporize. The vapor then travels through the adiabatic section, where it maintains a consistent temperature, to the condenser section. Here, the vapor releases its latent heat and condenses back into a liquid. The liquid returns to the evaporator through capillary action facilitated by a wick structure, thus completing a continuous cycle of efficient heat transfer.

Heat pipes can be categorized based on their working principles and structural features. Some of the types are conventional heat pipes, variable conductance heat pipes, vapor chambers heat pipes, diode heat pipes, rotating heat pipes, capillary pumped loop heat pipes and grooved heat pipes [3]. The primary components of a heat pipe include the working fluid and the wick structure. The working fluid, selected based on properties like boiling point and thermal conductivity, undergoes phase changes to transfer heat. The wick structure, lining the inside of the pipe, facilitates the return of the condensed liquid to the evaporator through capillary action [4].

Heat pipes offer numerous advantages, including: high thermal conductivity and efficient heat transfer over long distances, passive heat transfer, uniform temperature distribution and minimal thermal strains, versatility in orientation and long operational life [5]. Hence, they are integral in variety of applications such as electronic cooling, medical devices, energy systems, HVAC and Refrigeration, Battery Thermal Management, high performance Computing and

Military & Defense Systems [6]. Heat pipes operate within certain limits, which include: sonic limit, entrainment limit, capillary limit, boiling limit and viscous limit [7]. Understanding these limits is crucial for optimizing heat pipe design and ensuring effective thermal management across various applications.

2. LITERATURE REVIEW

The development and optimization of heat pipe systems have seen significant progress over recent years, with numerous studies focusing on various aspects of heat pipe performance, design, and application by various researchers and scholars. This literature review aims to provide a chronological overview of the key advancements in this field, highlighting the connections between different research efforts to present a cohesive narrative of the evolving technology.

Kumar et al. [8] conducted a foundational study on optimizing heat pipe parameters, identifying internal pressure as the most critical factor for effectiveness, followed by fluid filling ratio, inclination, and number of wick layers. Their empirical model demonstrated the optimal combination of a 40% filling ratio, 0.2 bar pressure, 2 wick layers, and 0-degree inclination. Expanding on this, Bhatt et al. [2] investigated AGMBHP for different filling ratios and orientations under equal and unequal heat loads. They found that the horizontal orientation was optimal, enabling the heat pipe to transmit a 240 W heat load with minimal resistance. This study highlighted the importance of orientation and dynamic characteristics in heat pipe performance. In a subsequent study, Bhatt et al. [9] examined wickless multi-branch heat pipes, focusing on start-up and dynamic characteristics. They discovered that the optimal filling ratio varied with heat load, demonstrating the flexibility of multi-branch thermosiphon heat pipes to handle significant heat loads with low thermal resistance.

Shah et al. [10] employed modeling and parametric analysis for loop heat pipes (LHPs) using Dev-C++ software. Their results, validated against existing literature, showed that condenser effectiveness and wick porosity significantly impacted LHP performance, emphasizing the importance of these parameters in design. Addressing heat transport limitations, Patrik N. et al. [7] developed a mathematical model for calculating limitations across different wick structures and working fluids. Their findings provided valuable guidelines for designing heat pipes operating across a wide temperature range.

Hammad [11] explored solar energy applications, detailing the performance of flat plate solar collectors cooled by heat pipes. This study demonstrated the efficiency of heat pipes in low-temperature conditions, comparing favorably with traditional water-cooled collectors.

Hongting et al. [12] integrated thermodynamic principles to identify optimal operational conditions for slag cooling using water-water heat pipe heat exchangers (HPHE). Their research underscored the effectiveness of an online cleaning device in enhancing heat transfer. Kim et al. [13] compared water-filled heat pipes with those filled with SiC/water nanofluids and SiC-coated wicks. They found that while nanofluids did not improve performance, SiC-coated heat pipes showed higher wall temperatures, influencing heat transmission. Ying et al. [14] introduced phase change materials (PCM) in heat pipes for electronic cooling. Their experiments revealed significant fan power savings with tricosane as PCM, highlighting the potential of PCM in thermal management.

Shi et al. [15] analyzed variable conductance heat pipe air preheaters, confirming their anti-corrosion and anti-ash-deposition performance in industrial applications, demonstrating robustness under varying conditions. Mingke et al. [16] compared wick and wickless heat pipe PV/T systems, recommending specific systems based on latitude. Their research provided practical guidelines for optimizing the thermal efficiency of PV/T systems. Joseph and Young [17] studied the thermal hydraulic characteristics of long heat pipes, focusing on the entrainment limit's sensitivity to the length-to-inner-diameter (L/D) ratio. They developed a modifying factor that accurately correlated experimental results.

Sihui et al. [18] investigated ULHPs using air cooling for condensation, identifying optimal conditions for minimal thermal resistance and effective operation under varying heat loads. Deqiang et al. [19] focused on ultra-thin flat heat pipes, finding that a 15% liquid filling rate offered the smallest thermal resistance, contributing to design optimization for minimal thermal resistance applications. Pekur et al. [20] examined gravity heat pipes with threaded evaporators, demonstrating their effectiveness in

natural air-cooling systems for high heat flux electronic equipment. Tianling et al. [21] reviewed small heat pipes, discussing advancements in materials and fabrication processes. They highlighted the potential of nano wicks and affordable fabrication techniques for future small heat pipes.

Orr et al. [22] reviewed waste heat recovery systems in internal combustion engines, identifying thermoelectric generators (TEGs) and heat pipes as promising technologies for improving automotive efficiency. Ling et al. [23] focused on heat pipe applications in data centers, discussing how working fluid type and geometrical parameters influence thermal performance, providing insights for large-scale electronic cooling. Nakamura et al. [24] evaluated gravity effects on long-distance loop heat pipes (LLHPs), finding that anti-gravity effects influenced vapor blanket formation and heat transport efficiency. Zhang et al. [25] explored heat recovery properties of a flat micro-heat pipe array using nanofluids, demonstrating significant enhancement in heat recovery efficiency with specific nanofluid concentrations.

In summary, these studies collectively advance our understanding of heat pipe technologies, highlighting the importance of optimizing various parameters to enhance performance across different applications. From electronics cooling and solar energy systems to industrial heat exchangers and automotive waste heat recovery, heat pipes continue to demonstrate their versatility and efficiency in thermal management [8-25].

3. EXPERIMENTAL SETUP & METHODOLOGY

3.1 Experimental Setup

The schematic diagram of the experimental setup is shown in Fig. 1(a). The heat pipe was fixed inside the stainless-steel shell such that the evaporator and adiabatic sections remained outside the shell and the condenser section inside the shell. A helical shaped heater was provided on the evaporator section of the heat pipe for the heat input. The shell was fixed on the stand and an arrangement was made to change the inclination of the heat pipe which was set as 45° in our case. In order to avoid heat losses from the shell to the surrounding, 25mm thick rockwool insulation was provided on the shell, the adiabatic section of heat pipe as well as the heater (which is provided on the evaporator section). The cooling water was circulated at the constant mass flow rate of 2.667ml/s through the shell over the condenser section. In order to maintain a constant head of water, a storage tank was provided with a stand. At inlet and outlet of the shell, flow control valves were provided for the flow regulation. For the temperature measurement, seven numbers of RTD sensors (PT 100) were provided along the axial direction of heat pipe as shown in Fig. 1(b). The photograph of the experimental setup is shown in Fig. 2(a). and the major specifications of different components and instruments are tabulated in Table 1.

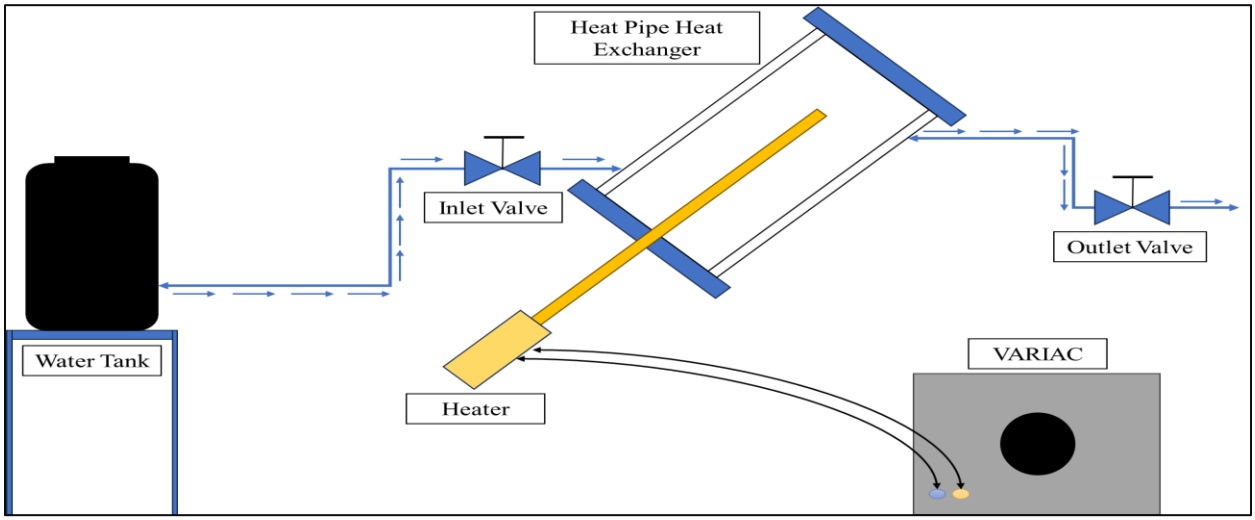

Fig. 1(a): Schematic diagram of the experimental setup

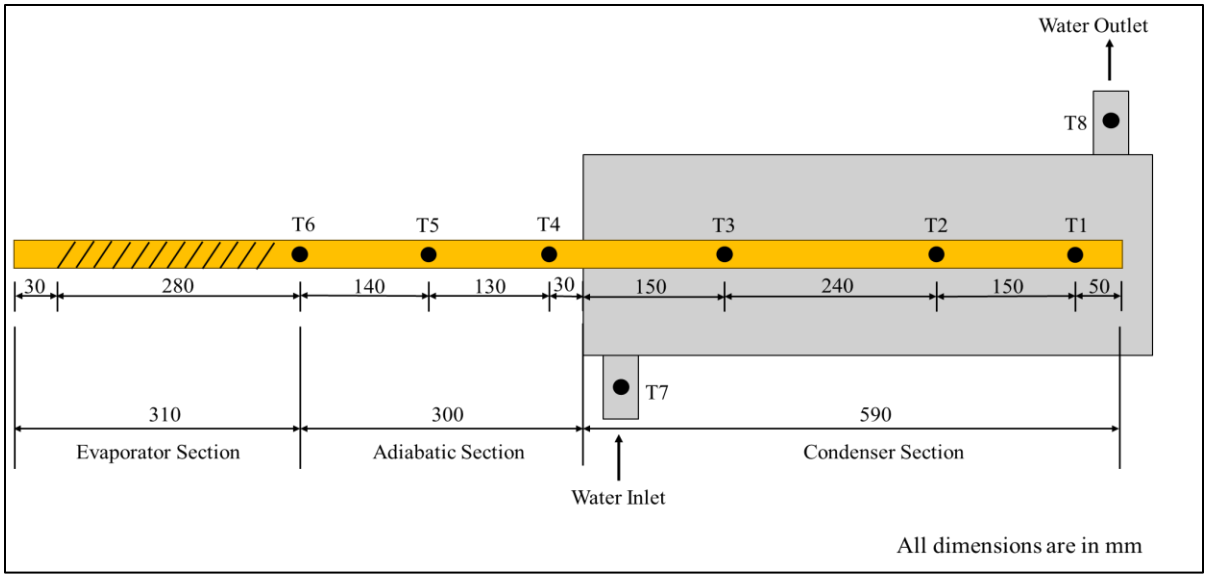

Fig. 1(b): Location of temperature sensors along the axial direction of heat pipe

The heat pipes used in the experiments were indigenously developed in the Advanced Heat Transfer Laboratory of Mechanical Engineering Department, Institute of Technology, Nirma University. For the fabrication of heat pipe, copper pipe (ID: 21.4mm, OD: 25.4mm) was selected. As a working fluid inside the heat pipe, distilled water was selected in view of its working range (30ºC to 200ºC) as well as its compatibility with copper [26]. Depending on the predefined filling ratio, the required quantity of distilled water was filled in the copper pipe. As a wick, stainless steel wick of 100 mesh size was used as shown in Fig. 2(b). In the present study, the experiments were performed at four different filling ratios viz. 20%, 30%, 40% and 50%FR under atmospheric pressure at different heat inputs.

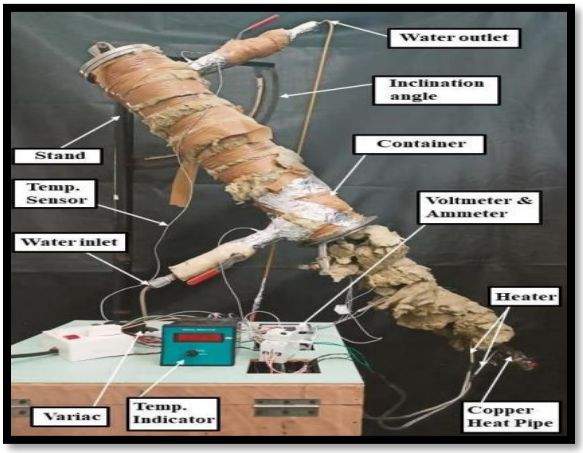

Fig. 2(a): Photograph of the experimental setup

Fig. 2(b): Photograph of the inserted SS wire wick in the heat pipe

Table 1: Major specifications of various components and instruments

Name of Component	Details	
Heat Pipe	Material: copper; ID: 21.4 mm	OD: 25.4 mm; Length: 1.2 m
Shell	Material SS 304; ID:108 mm	OD: 114mm; Height: 700 mm
Heater	Shape: Helical	Capacity: 1 kW
Wick	Material: SS; Mesh Size:100 1 wick	Wire dia.: 0.11 mm Opening width: 0.14 mm
Insulation	Material: Glass wool	Thickness: 25 mm
Water tank	Capacity: 1000 lit	
RTD sensors	Type: PT100 Range: -99 °C to 400 °C	Least count: 0.1 V
Variable autotransformer	Range: 0-250V	Least count: 1 V

All the measuring instruments were calibrated prior to their application in the experimentation. The uncertainty in various performance parameters was estimated in accordance with the procedure given by Kline and McClintock [27]. The details of uncertainty analysis carried out for the various parameters are given in appendix 1. The relative uncertainty in overall thermal resistance (R_o), overall heat transfer coefficient (h_o), heat supplied to the evaporator section (Q_e), heat gained by the cold water (Q_c) and efficiency of heat pipe (Ƞ) were estimated to be 2.60%, 1.33%, 2.58%, 0.21% and 2.59% respectively.

3.2 Methodology

We begin the experiment by attaching temperature sensors to the heat pipe using M-seal. Then, the heat pipe is carefully placed inside the condenser section. Next, a heater is securely fastened to the evaporator section of the heat pipe. To monitor the heat transfer process, temperature sensors are installed at both the inlet and outlet of the condenser's water flow. To minimize heat loss during the experiment, the heat pipe is meticulously insulated with glass wool. Once the setup is complete, the system is configured to achieve the desired mass flow rate for the cooling water. Finally, temperature readings are taken. During the initial 10 minutes, where a rapid temperature increase is expected, readings are recorded every 2 minutes. Following this initial phase, readings are taken at 10-minute intervals for continued monitoring.

3.3 Performance parameters

The heat pipe performance was evaluated by considering different parameters such as thermal resistance, heat transfer coefficient, efficiency of the heat pipe and the effective thermal conductivity.

Thermal Resistance: Thermal resistance plays an important role in heat transfer within the heat pipe. If the thermal resistance is small, heat transfer will be better and vice versa. The thermal resistances of evaporator and condenser sections and the overall thermal resistance of heat pipe were evaluated using the following equations [13][28]

$$R_e = \frac{(T_e - T_a)}{Q} \quad (1)$$

$$R_c = \frac{(T_a - T_c)}{Q_c} \quad (2)$$

$$R_o = \frac{(T_e - T_c)}{Q} \quad (3)$$

where, T_e, T_a and T_c are the average wall temperatures of evaporator, adiabatic and condenser sections (°C). In order to obtain T_e, T_a and T_c, the wall temperatures were recorded with time along the length of the heat pipe (in the axial direction). The steady state readings were used to evaluate these temperatures.

Q is the heat supplied to the evaporator section and Q_c is heat transferred to the cold fluid passing through the condenser section and are evaluated as under:

$$Q = V \cdot I \quad (4)$$

$$Q_c = \dot{m} \cdot C_p \cdot (T_{co} - T_{ci}) \quad (5)$$

In the above equations, V and I are Voltage (V) and Current (A) supplied to the heater provided on evaporator section, $\dot{m}$ is the mass flow rate (kg/s) of water through the shell, C_p is specific heat capacity of cooling water (kJ/kg-K), T_{ci} and T_{co} are the cooling water inlet and outlet temperatures (°C) in the condenser section.

Heat transfer coefficient: The heat transfer characteristics of the evaporator and condenser sections were studied in terms of the heat transfer coefficient. The heat transfer coefficients for evaporation and condensation and the overall heat

transfer coefficient were evaluated using the following equations [13][28]

$$h_e = \frac{Q}{A_e}(T_e - T_a) \quad (6)$$

$$h_c = \frac{Q_c}{A_c}(T_a - T_c) \quad (7)$$

$$h = \frac{Q}{A}(T_e - T_c) \quad (8)$$

where, A_e, A_c and A refers to the area (m^2) of the evaporator section, condenser section and entire heat pipe respectively.

Efficiency of the heat pipe: The performance of heat pipe was analyzed in terms of efficiency (Ƞ) as defined below.

$$\eta = \frac{Q_c}{Q} \quad (9)$$

where, Q and Q_c refers to the heat supplied to the evaporator section and heat transferred to the cold fluid passing through the condenser section respectively.

Effective Thermal Conductivity: The thermal conductivity of the heat pipe attributes to the ability of the heat pipe to transfer heat efficiently. The effective thermal conductivity of the heat pipe was evaluated using the below equation [3]

$$k_e = \frac{(Q \cdot L_{eff})}{A_c \Delta T} \quad (10)$$

where,

$$L_{eff} = \frac{(L_{evap} + L_{cond})}{2} + L_{adia} \quad (11)$$

In the above equations, Q refers to the heat supplied to the evaporator section (W), $L_{eff.}$ is the effective length of heat pipe (m), A_c is the area of the condenser section (m^2) and ΔT is the temperature difference between evaporator and condenser section (°C). Furthermore, in the calculation of $L_{eff.}$, L_{evap}, L_{adia} and L_{cond} refers to the length of evaporator, adiabatic and condenser section respectively.

4. RESULTS AND DISCUSSION

In this section, the effects of fluid filling ratio are discussed on the performance of axial heat pipe. The temperature variation along the axial direction of heat pipe as well as the variations in thermal resistances, effective thermal conductivity and heat transfer coefficients are also discussed.

4.1 Temperature distribution along the length

The steady state temperature distributions along the length of the axial flow heat pipe at different heat loads with different filling ratios are shown in Figs. 4(a)-4(d). It was observed that temperature decreased along the length of the heat pipe in all cases. As expected, the maximum temperature was found in the evaporator section and then decreased further along the condenser section. At 600W heat load with 40% filling ratio, the heat pipe was subjected to a minimum temperature variation along the length. At a lower filling ratio, a faster vapor generation rate makes the heat pipe quick responsive. However, for higher filling ratio, more heat is required to generate vapor which subsequently makes the heat pipe slow respondent and the axial conduction loss through the wall surface which in turn increases the temperature variation along the length. Similar trends of the temperature variation along the length of heat pipe were found with different filling ratios by Bhatt A. et al. in [2].

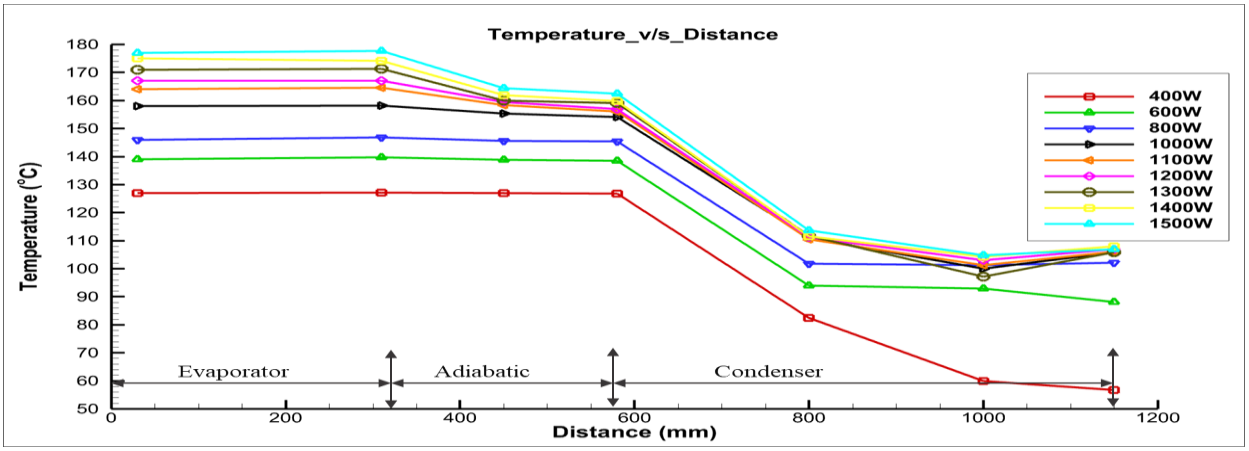

Fig. 4(a): Temperature profile of heat pipe for variable heat inputs at 20% filling ratio

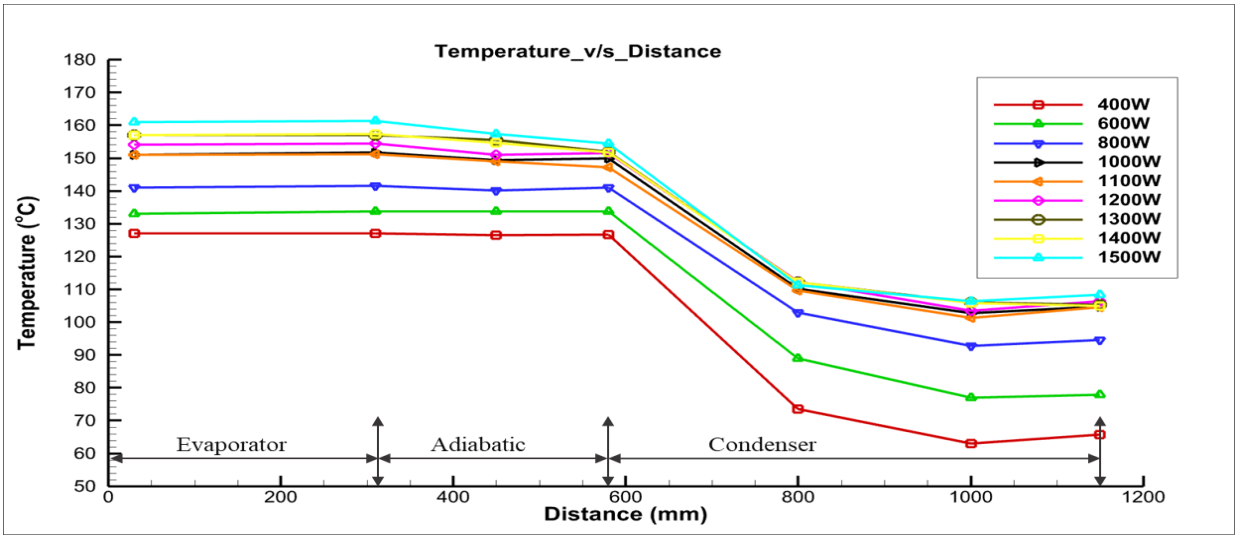

Fig. 4(b): Temperature profile of heat pipe for variable heat inputs at 30% filling ratio

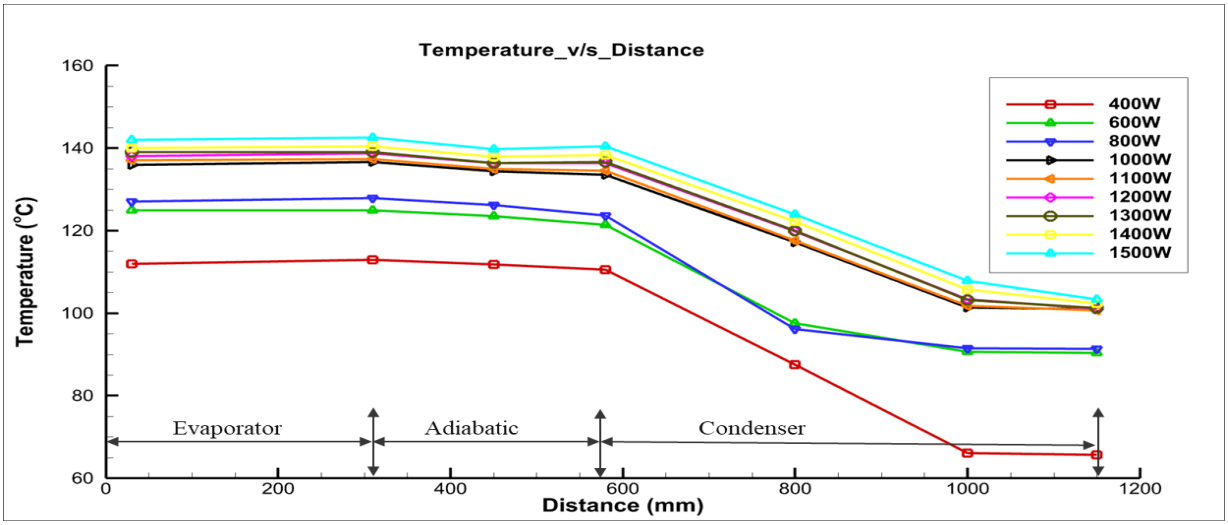

Fig. 4(c): Temperature profile of heat pipe for variable heat inputs at 40% filling ratio

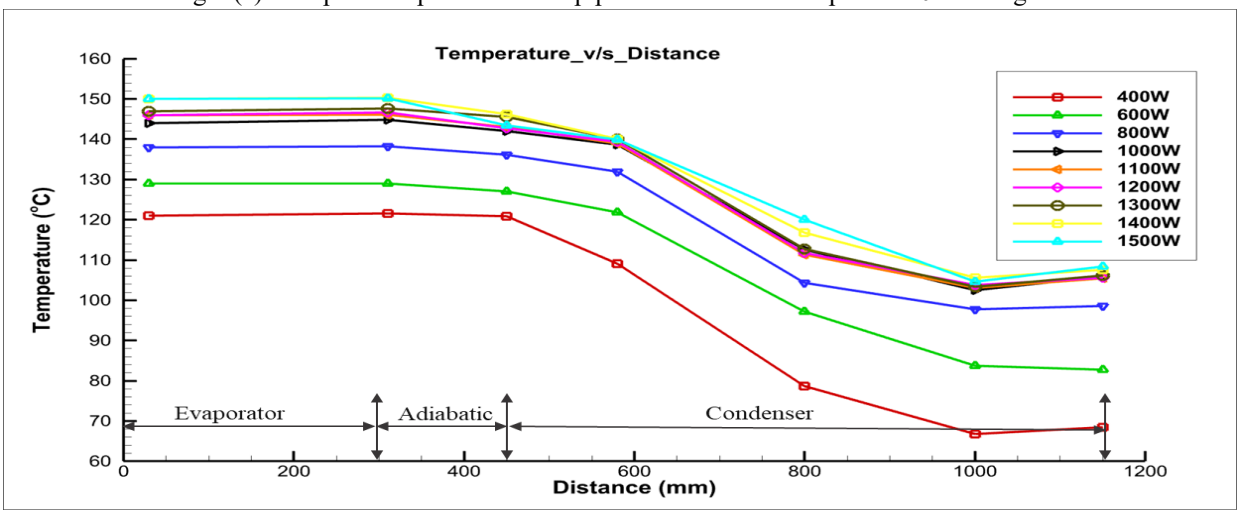

Fig. 4(d): Temperature profile of heat pipe for variable heat inputs at 50% filling ratio

The steady state temperature distributions along the length of the axial flow heat pipe at different filling ratios with three different heat inputs are shown in Figs. 5(a)-5(c). For an ideally conducting heat pipe the temperature indicators at all the locations should read the same reading, i.e., there should be zero thermal resistance in the heat pipe. But due to resistance in the vapor flow, imperfections in the capillary actions, impractical isothermal operation and material limitations, it is impossible to have an ideal heat pipe heat exchanger device. For the present range of 400-1500W the temperature profile of the heat pipe for minimum heat input, average heat input and maximum heat input was discussed in Figs. 5(a)-5(c). For all the heat inputs the best possible results were observed for 40% filling ratio. The maximum possible temperature difference in minimum, average and maximum heat input was obtained as 70.4 °C, 63.2 °C and 72.9 °C, respectively. At a given filling ratio with less working fluid, the temperature difference between evaporator and condenser section is small, but the heat transfer is poor. As the optimum filling ratio is reached, there's enough working fluid for efficient evaporation and transport leading to clear temperature gradient along the heat pipe. Further, increasing the working fluid leads to blocking of internal channels and reduced heat transfer and more temperature difference is hence obtained. Also, it can be observed from the Figs. 5(a)-5(c), there is a sudden drop as we move from adiabatic to condenser region due to the fact that the heat removal takes place at the condenser region.

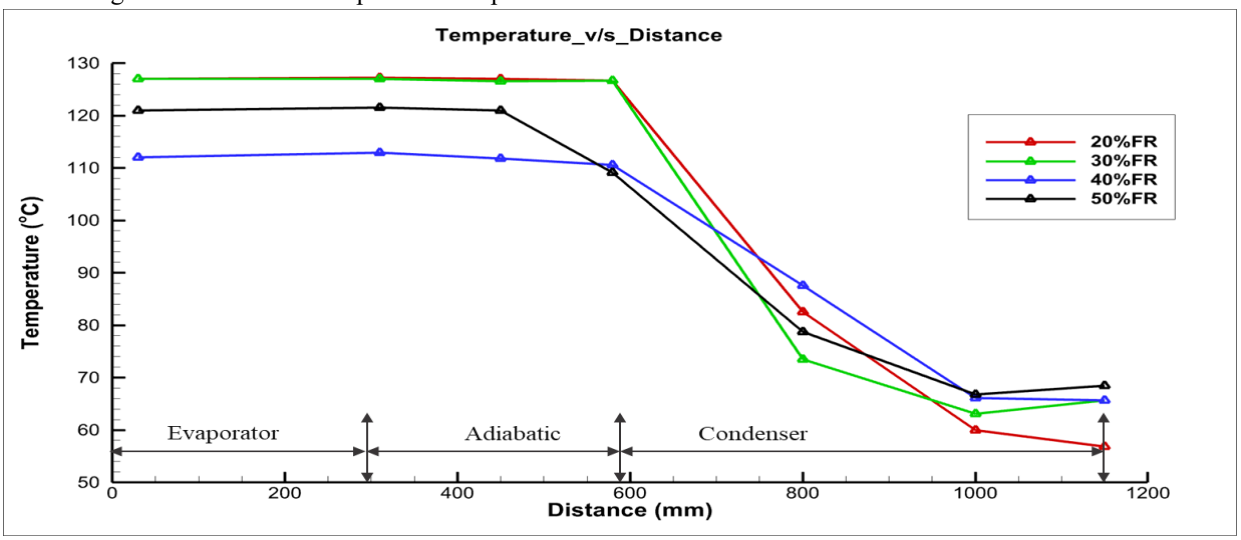

Fig. 5(a): Temperature profile of heat pipe at minimum heat input for different filling ratios

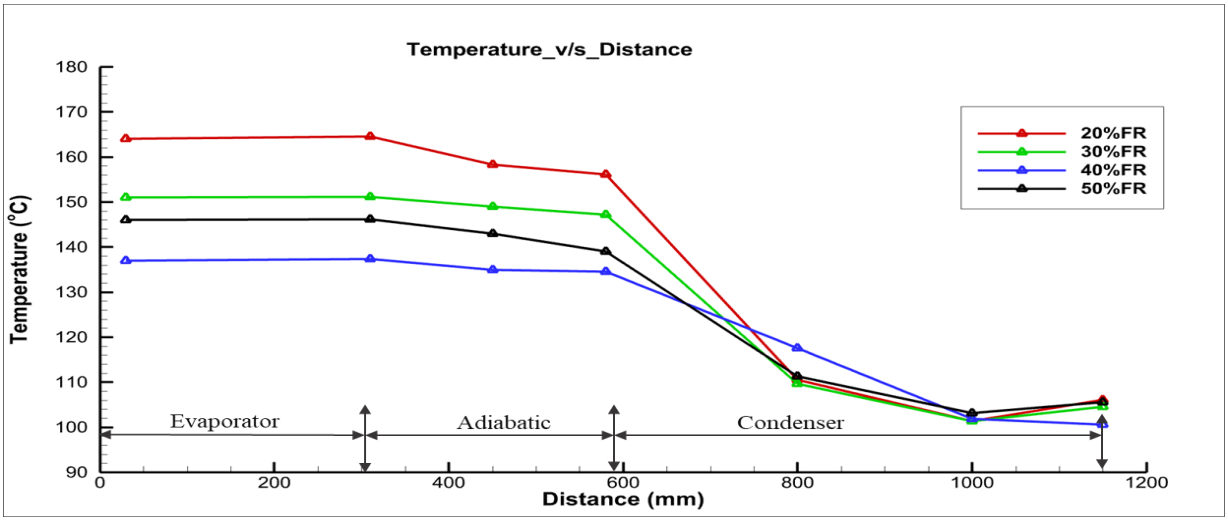

Fig. 5(b): Temperature profile of heat pipe at average heat input for different filling ratios

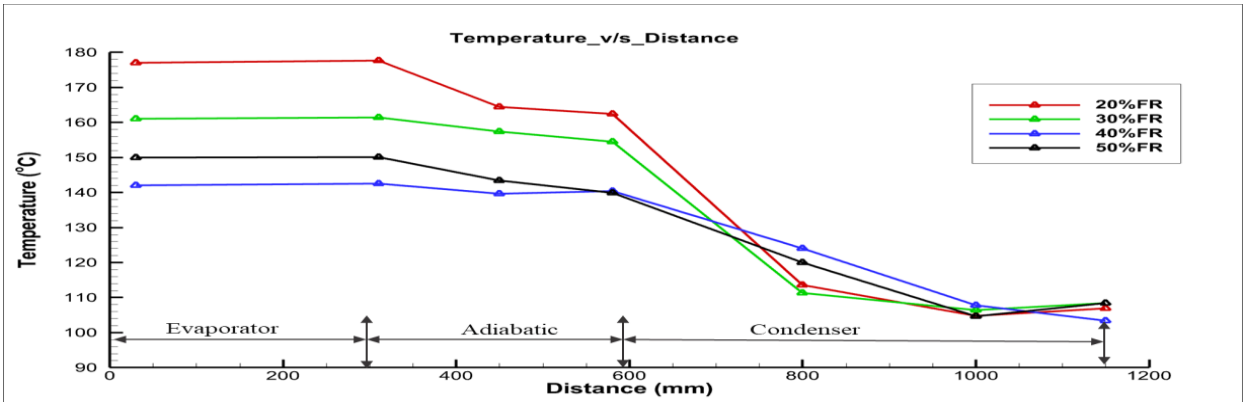

Fig. 5(c): Temperature profile of heat pipe at maximum heat input for different filling ratios

4.2 Variation in Temperature of different sections

The filling ratio is one of the most important parameters affecting the thermal performance of the heat pipe. In the present study, the wicked heat pipe, the filling ratio was considered as the ratio of the filled volume of the working fluid to the total available filling volume of the heat pipe. It is required to optimize the filling ratio because the smaller filling ratio may result in an early dry-out of the heat pipe at higher heat inputs, whereas an excessive amount of filling ratio may prevent the vapor flow path. In this study, the experiments were performed with four different filling ratios namely, 20%, 30%, 40% and 50%. As shown in Fig. 6(a), with an increase in the heat load, the surface temperature of the evaporator section, adiabatic section and the condenser section increased. Moreover, the temperature difference between the evaporator and condenser first decreases reaches up to an optimum point and then increases in the case of 20%, 30% and 50% filling ratios as practically it is not possible to obtain a zero thermal resistance. While the lowest difference was reported as 30.4°C at 1400W and 40% filling ratio. The lower temperature difference indicates lower thermal resistance and an effective heat transfer.

For lower filling ratio, with an increase heat load, boiling of water and generation of vapor occur at comparatively higher rate. The presented heat pipe geometry is such that in which liquid working substance from the condenser can be visualized to fall under the effect of gravity. However, in this motion of liquid return, it also encounters vapor from opposite direction. Basically, at lower filling ratio, there may not be enough amount of liquid to guarantee effective boiling, as the length of heater is more than the length of fluid column contained within the pipe, even after sufficient condensation. As the filling ratio increases, sufficient water is available in the evaporator section for the phase conversion. If the filling ratio is increased further, the excess water present in the evaporator section will start to obstruct the flow path of vapor affecting the heat transfer rate of heat pipe.

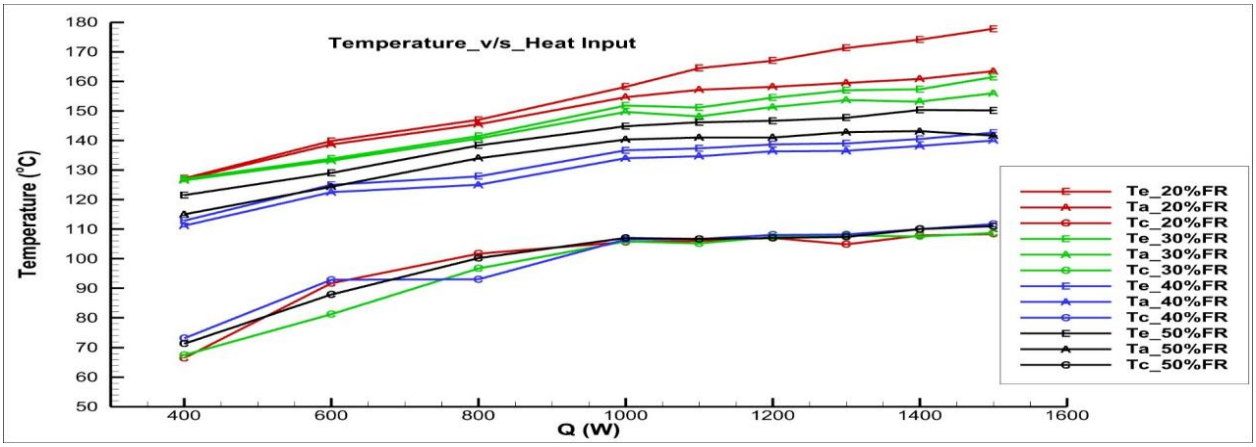

Fig. 6(a): The variation of temperatures along different sections at variable heat inputs for different filling ratios

Consequently, the inlet water, outlet water and the difference between inlet and outlet water flowing through the condenser section are shown in Fig. 6(b). The inlet water temperature resembles the ambient temperature as the source of it is the overhead water tank. In the parallel flow mechanism of this heat exchange device, the temperature of the water rises as it passes from one end to the another. Further, with an increase in heat load the outlet temperature is increased and the difference between both (inlet and outlet) is increased.

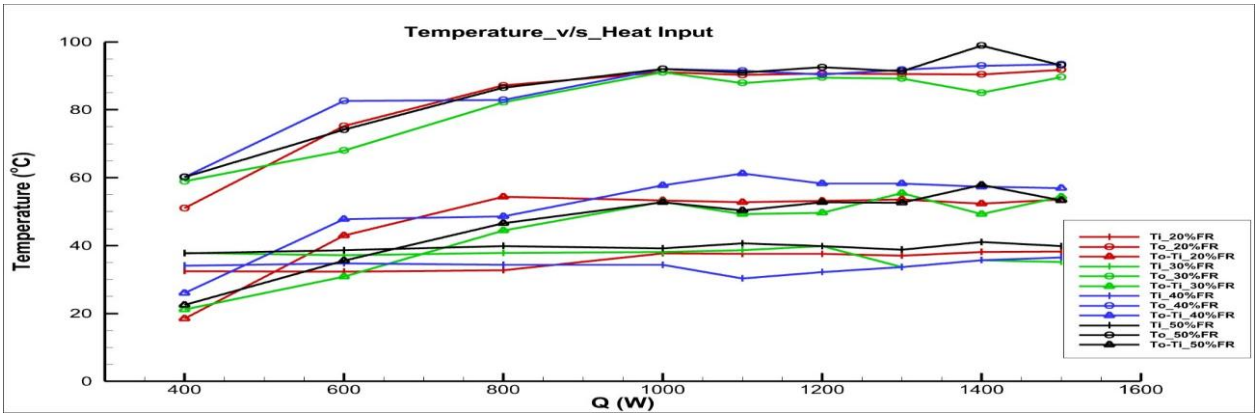

Fig. 6(b): The change in water temperatures at variable heat inputs for different filling ratios

4.3 Variation in the Heat transfer coefficient

The convective heat transfer coefficient of the evaporator section, condenser section and total heat transfer coefficient of heat pipe were calculated using the Eqs. (6), (7) and (8) respectively. Figs. 7(a)-7(b) show the variation of these at different heat loads with different filling ratios. Heat transfer co-efficient at evaporator section is denoted as “he”, at condenser section is denoted as “hc” and overall heat transfer co-efficient is denoted as “h”, respectively. Initially, when the heat load is low, there is insufficient heat to cause water evaporation. As a result, the majority of the heat is primarily conducted by the copper pipe. As the heat load increases, reaching a sufficient level, a larger portion of heat is carried away by water vapor. On account of the filling ratio, at lower filling ratio, there is not enough working fluid to efficiently transfer heat. Hence, the vapor space dominates, and the circulation becomes sluggish. As the filling ratio is increased, the heat transfer rate as well as the coefficient of heat transfer increases. If the filling ratio is increased further, in the case of 50% filling ratio, excessive liquid can flood the wick structure and hinder the vapor flow, thus reducing the heat transfer or even entrainment of heat pipe can occur. The analysis concluded that the 40% filling ratio provides the highest value of convective heat transfer coefficient (507.75 W/m^2-K) at 1400 W compared to other filling ratios of heat pipe.

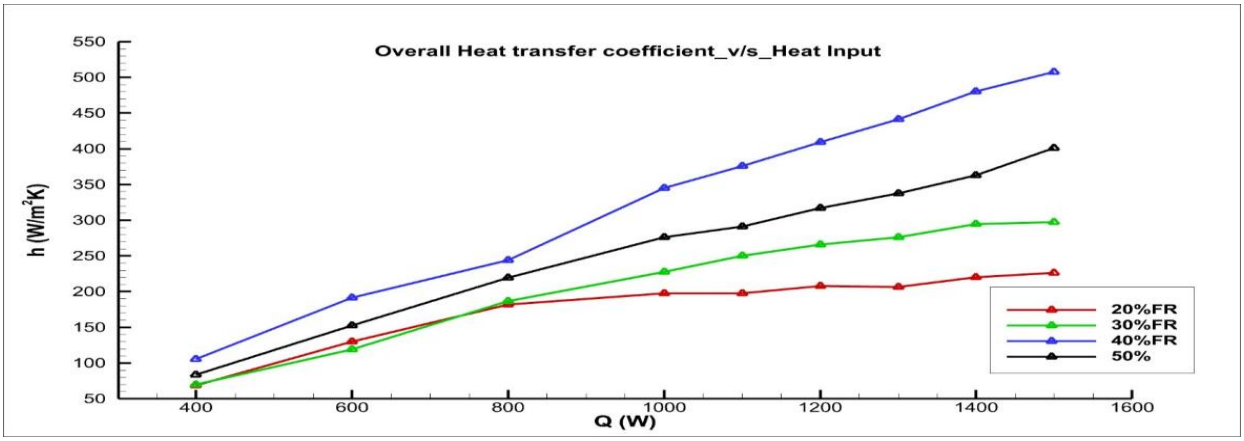

Fig. 7(a): The change in convective heat transfer coefficient at variable heat inputs for different filling ratios

It was observed that the maximum heat transfer coefficient for heat pipe is obtained where thermal resistance is minimum. Moreover, the results obtained here for variation of heat transfer coefficient also validate the thermal resistance results described in Fig. 8(a). From Figs. 7(a)-7(c), it is evident that evaporator heat transfer coefficients are maximum for a particular heat load for each filling ratio. This is due to the fact that for each quantity of working substance, a particular heat load provides the most effective phase change in the evaporator. From Fig. 7(b), it was observed that for lower filling ratio, 20% and 30% filling ratio, the convective heat transfer coefficient of evaporator decreased rather than increasing. This is attributed to the fact that for lower filling ratio in the case of thermosiphon heat pipe, there is a shift in boiling regime from nucleate to film boiling in the evaporator. The boiling in the evaporator can be considered as pool boiling and when the amount of working fluid is less, then the heat supplied by the heater present at the evaporator section is absorbed by the vapor rather than the working fluid as all the fluid is converted into vapor. The vapor then becomes superheated and further the heat transfer is insufficient. Hence, as the amount of heat input increases the convective heat transfer coefficient of evaporator decreases. Similar trends were also reported by Guichet et al. [29].

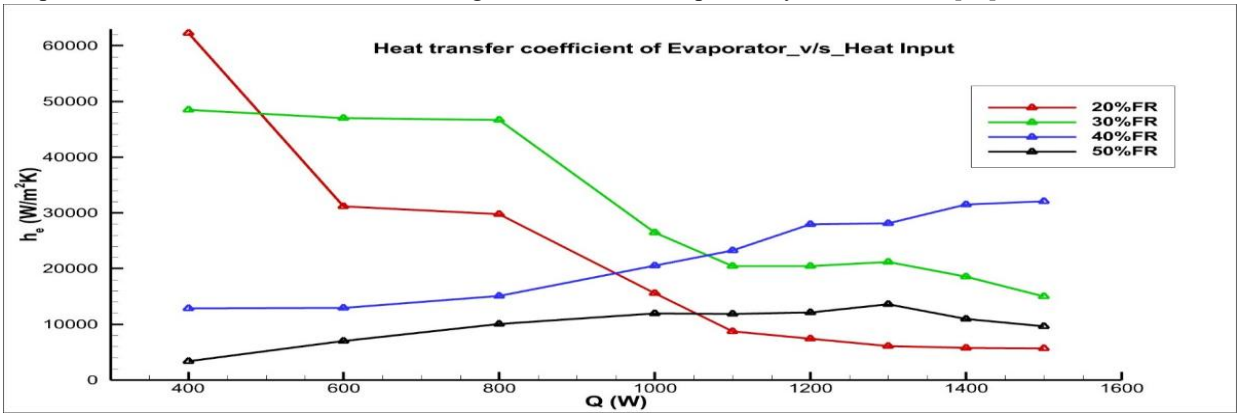

Fig. 7(b): The change in heat transfer coefficient of evaporator section at variable heat inputs for different filling ratios

Variation in heat transfer coefficient of condenser with respect to the heat load at different filling ratio is shown in Fig. 7(c). As the heat input at the evaporator section is increased the heat transfer coefficient of condenser section first increases, reaches up to an optimum point and then decreases. It was found that the heat transfer coefficient of condenser section varied from maximum (overall) 533.689 W/m^{2}K to minimum (overall) 238.384 W/m^{2}K (Fig. 7(c)). For input range of 400-1000W, the vapor flow is easier in the case of 20% filling ratio and hence the convective heat transfer coefficient of condenser is more for 20% filling ratio in this working range.

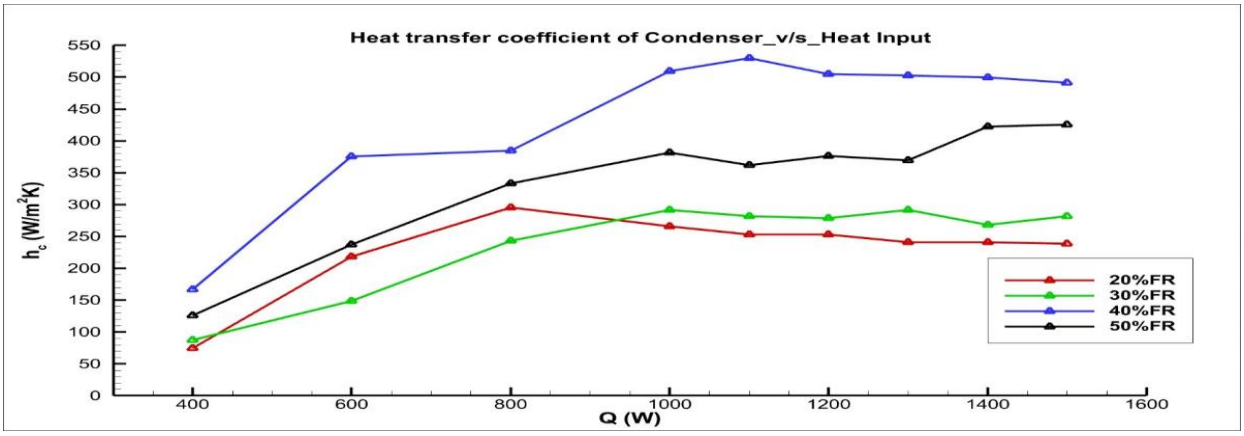

Fig. 7(c): The change in heat transfer coefficient of condenser section at variable heat inputs for different filling ratios

4.4 Variation in the Thermal resistance

One of the methods of studying the effect of the filling ratio on the heat pipe performance is to evaluate the total thermal resistance between evaporator and condenser. The total thermal resistance of the heat pipe was calculated using the Eq. (3). The separate thermal resistances of evaporator and condenser sections were calculated using Eqs. (1) and (2), respectively as described earlier. Variation in total thermal resistance, evaporator thermal resistance, and condenser thermal resistance with respect to the heat load at different filling ratio are shown in Figs. 8(a)-8(c). It was found that the total thermal resistance varied from maximum (overall) 0.152 °C/W to minimum (overall) 0. 0.0205 °C/W (Fig. 8(a)). The results also validated the analysis as described in section 4.3.

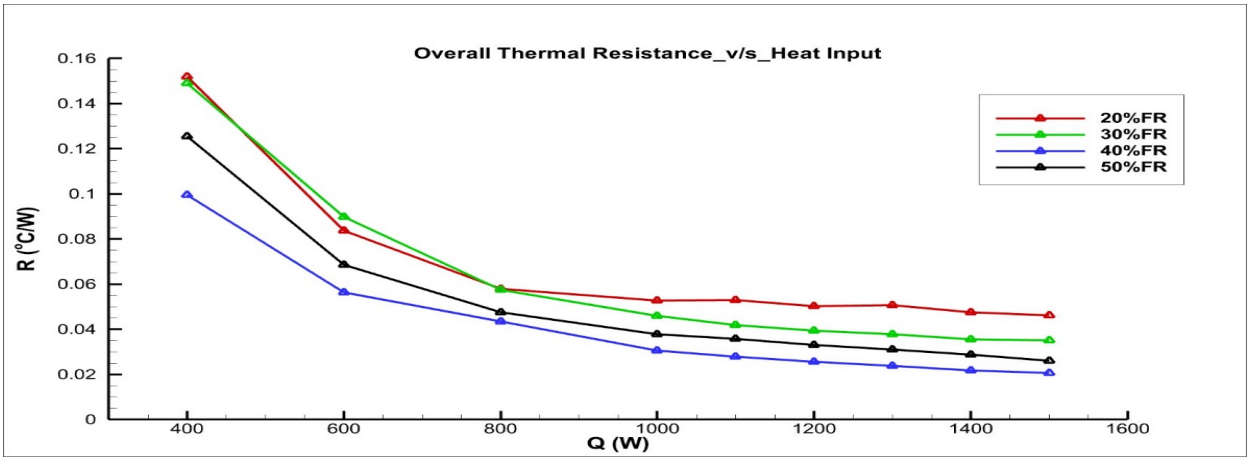

Fig. 8(a): The change in overall thermal resistance at variable heat inputs for different filling ratios

It was found that the evaporator thermal resistance (Fig. 8(b)) varied from the maximum of 0.000953 °C/W to the minimum of 0.000875 °C/W with 20% filling ratio, 0.0036 °C/W to 0.001125 °C/W with 30% filling ratio, 0.00425–0.0017 °C/W with 40% filling ratio, and 0.01625–0.00563 °C/W with 50% filling ratio. It was observed that for the lower values of heat loads, thermal resistances are very large compared to higher heat loads in all the cases. With an increase in the heat load, the vapor generation rate, pressure, and the movement of working fluid also increased, which gradually decreased the resistance of the heat pipe. However, an increment of heat load beyond a certain limit may cause evaporator dry-out due to local attainment of the boiling limit. Moreover, in the present working range of 400–1500 W, the evaporator resistance was found to be lower than 0.01888 °C/W for all the filling ratios.

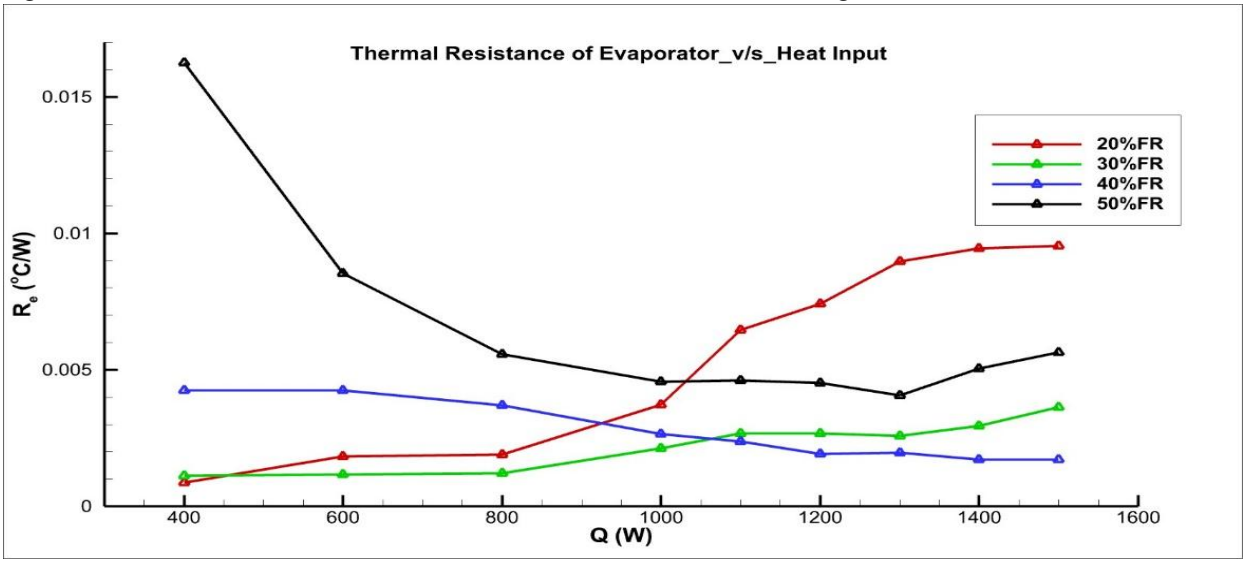

Fig. 8(b): The change in thermal resistance of evaporator section at variable heat inputs for different filling ratios

It is clear from Fig. 8(c), the condenser thermal resistance gradually decreased with an increase in heat load. The maximum condenser resistance was found below 0.3 °C/W for all the filling ratios. The average value of condenser resistance was found to be lower than that of average evaporator resistance and also there was sufficient cooling of vapor in the condenser. The minimum total thermal resistance point is achieved at 40% filling ratio and 1400W heat load in Fig. 8(a), so this combination of heat load and filling ratio can be considered as optimum for proposed heat pipe under tested conditions. Thermal resistance for the given filling ratio of the heat pipe can be visualized as how effectively the working substance absorbs the given amount of heat and undergoes phase change rather than wall conduction. Large thermal resistance means a large fraction of wall conduction and poor phase change. It is a well-established fact that at a small value of heat load, the rate of vapor generation is small which may slow down the phase change (evaporation–condensation) cycle and increases thermal resistance. The same can be observed in Fig. 8(a) at a low value of heat loads for all filling ratios. Further, if the quantity of the working substance is more than the optimum for given small value of heat load, then the phase change may be further poor in order to heat large bulk of the working substance. Which is the case observed in Fig. 8(a) for 50% filling ratio.

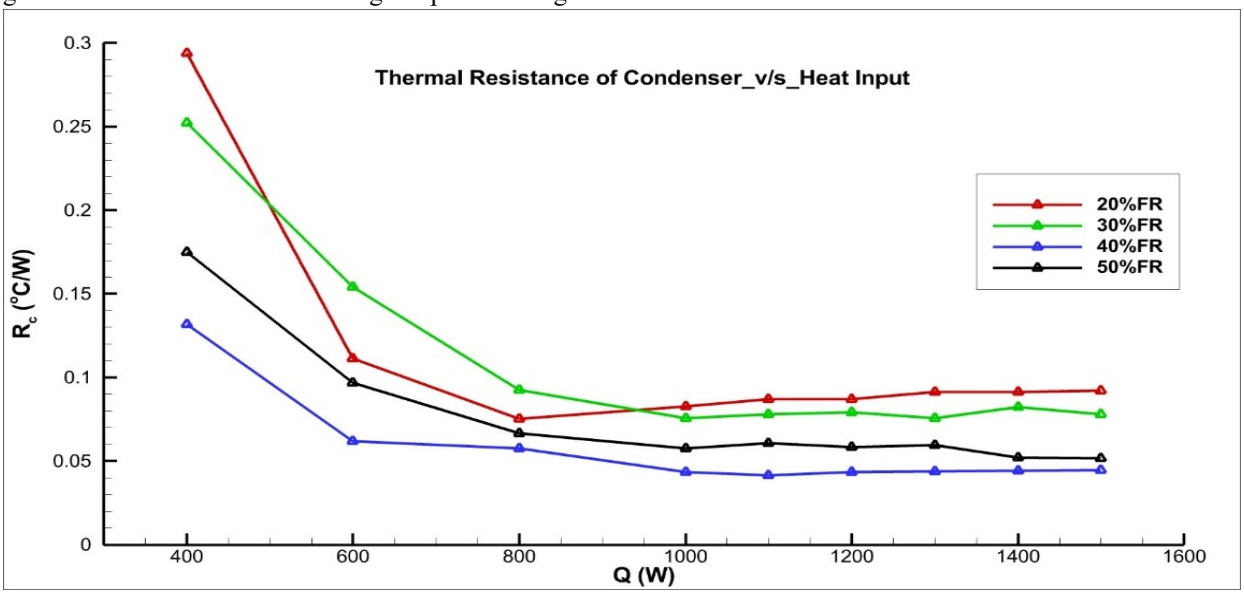

Fig. 8(c): The change in thermal resistance of condenser section at variable heat inputs for different filling ratios

4.5 Variation in Overall Thermal Efficiency

One of the important performance parameters of studying the effect of the filling ratio on the heat pipe performance is by evaluating the thermal efficiency of the heat pipe. The thermal efficiency of the heat pipe was calculated using the Eq. (9). Variation in thermal efficiency of heat pipe with respect to the heat load at different filling ratio is shown in Fig. 9. It was found that the total thermal efficiency varied from maximum (overall) 88.54% to minimum (overall) 39.13% (Fig. 9). As shown in Fig. 9, the thermal efficiency increases with increase in heat input up to a certain limit and then decreases. This accounts for the fact that as we increase the heat input, more vapor is generated in the evaporator section and an increased vapor flow enhances the heat transfer. Then it reaches an optimum point where there's enough liquid for efficient evaporation, and vapor flow isn't restricted. The heat pipe at this point operates at its peak efficiency, transferring heat with minimal thermal resistance. If the heat input is increased further, it can lead to dry out or flooding & pressure build (in case of higher filling volume) and hence reduce the efficiency of the heat pipe. The maximum efficiency is obtained at 600W and 40%filling ratio. Further, the trend of 20% filling ratio depicts that at 800W, 20% filling ratio provides optimum condition for heat transfer. This can be attributed to the sonic limit of the heat pipe. When the working fluid is less, heat waves can travel faster and more efficiently increasing the efficiency of the heat

pipe. Other than that, the 40% filling ratio provides optimum condition throughout the working range.

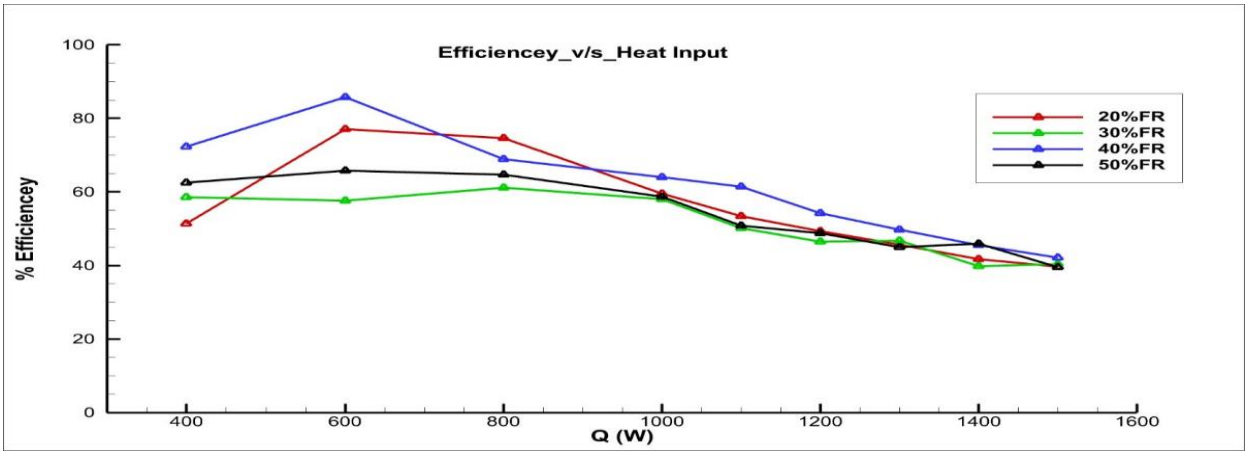

Fig. 9: The change in the thermal efficiency of the heat pipe at variable heat inputs for different filling ratios

4.6 Variation in Effective Thermal conductivity

Variation in the effective thermal conductivity of heat pipe with respect to the heat load at different filling ratio is shown in Fig. 10. The effective thermal conductivity of the heat pipe was calculated using the Eq. 10. The thermal conductivity of the heat pipe is crucial for its ability to transfer heat efficiently. Unlike a solid metal rod, a heat pipe has much higher effective thermal conductivity, i.e., it can transfer significantly more heat per unit area per degree of temperature difference. The values of the thermal conductivity ranges from 1,500 W/m-K to 50,000 W/m-K, compared to 400 W/m-K for copper. Since the heat pipe utilizes two phase heat transfer process involving a (evaporation-condensation) cycle, they exhibit superior thermal conductivity than ideal metal pipe. As shown in Fig. 10, for a given filling ratio, the effective thermal conductivity increases with an increase in the input power. Also, for the four different filling ratios, the highest thermal conductivity is obtained at 40% filling ratio. Further, it is observed that at low power input in the range of 400-800W, conductivity of 20% filling ratio is better than 30%. This again attributes to the same fact that due to the significance of sonic limit of heat pipe in this case, heat waves travel faster due to less filling ratio. It was found that the effective thermal conductivity varied from maximum (overall) 85.105 kW/m-K to minimum (overall) 12.637 kW/m-K (Fig. 10).

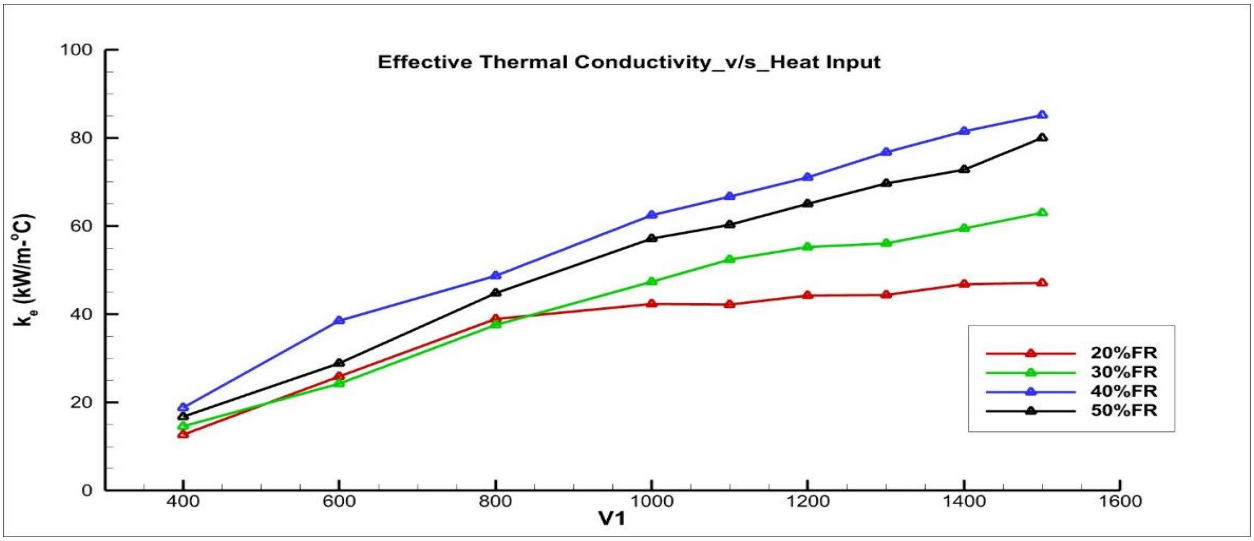

Fig. 10: The change in the effective thermal conductivity of the heat pipe at variable heat inputs for different filling ratios

5. CONCLUSIONS

In the present study, experimental investigations were carried out on Industrial size heat pipe at varying loads for 20%, 30%, 40% & 50% FR on the heat pipe. The results are analyzed in terms of thermal resistance, heat transfer coefficient, effective thermal conductivity, and efficiency. The major conclusions drawn from the study are as under:

- The optimum filling ratio was determined to be 40%, resulting in a peak value of overall heat transfer coefficient of 507.758 W/m2 °C when subjected to 1500 W of power.
- The maximum heat flux was found to be 264892.429 W/$m2$ at 1500 W for 20% FR.
- The minimum thermal resistance observed in the heat pipe was 0.0206 °C/W at 1500 W with a filling ratio of 40%.
- The highest efficiency recorded was 88.5% with a 40% filling ratio and a single wick layer when subjected to 600W of power.

Nomenclature

T_e	Temperature of Evaporator section, ^oC
T_a	Temperature of Adiabatic section, ^oC
T_c	Temperature of Condenser section, ^oC
A_e	Area of Evaporator, m^2
A_c	Area of Condenser, m^2
C_p	Specific heat at constant pressure, kJ/kg-K
$\dot{m}$	Mass flow rate, kg/s
P	Pressure, Pa
Q	Heat supplied to the evaporator section, W
Q_c	Heat released at the condenser section, W
R	Overall thermal resistance, $^oC/W$
R_e	Thermal resistance of evaporator section, $^oC/W$
R_c	Thermal resistance of condenser section, $^oC/W$
h	Overall convective heat transfer coefficient, W/m^2-K
h_e	Convective heat transfer coefficient of evaporator section, W/m^2-K
h_c	Convective heat transfer coefficient of condenser section, W/m^2-K
k_e	Effective Thermal Conductivity, kW/m-K
Ƞ	Efficiency

REFERENCES

[1] A. Bhatt, S. V. Jain, R. N. Patel, and D. V. Vaghela, "Parametric Study on Axially Grooved Heat Pipe With Two Heat Sources and One Heat Sink With Multiple Branches," Journal of Thermal Science and Engineering Applications, vol. 15, no. 6, Apr. 2023, doi: https://doi.org/10.1115/1.4062155.

[2] L. L. Vasiliev, "Heat pipes in modern heat exchangers," Applied Thermal Engineering, vol. 25, no. 1, pp. 1–19, Jan. 2005, doi: https://doi.org/10.1016/j.applthermaleng.2003.12.004.

[3] Amir Faghri, Heat Pipe Science And Technology. Global Digital Press, 1995.

[4] P. D. Dunn and D. Reay, Heat Pipes. Elsevier, 2012.

[5] Bahman Zohuri, Heat Pipe Design and Technology Modern Applications for Practical Thermal Management. Cham Springer International Publishing, 2016.

[6] C. Dixon and P. Johnson, Heat Pipe Technology: Theory, Applications and Prospects. Pergamon, 1997.

[7] V. Kumar, S. V. Jain, Y. Shah, and V. J. Lakhera, "Parametric studies on interacting parameters influencing heat pipe performance," Proceedings of the Institution of Mechanical Engineers, Part A: Journal of Power and Energy, vol. 235, no. 3, pp. 594–607, Aug. 2020, doi: https://doi.org/10.1177/0957650920951100.

[8] A. Bhatt, S. Jain, and R. N. Patel, "Experimental Investigations on Performance Analysis of a Wickless Thermosiphon Heat Pipe With Two Heat Sources and Multiple Branches," Journal of Thermal Science and Engineering Applications, vol. 14, no. 10, Apr. 2022, doi: https://doi.org/10.1115/1.4054163.

[9] S. N. Shah, S. V. Jain, Kamlesh Kumar Baraya, and A. Madhusudan Achari, "Parametric Study on Ammonia-Based Loop Heat Pipe," Heat Transfer Engineering, vol. 44, no. 19, pp. 1775–1788, Nov. 2022, doi: https://doi.org/10.1080/01457632.2022.2148347.

[10] "Mathematical model for heat transfer limitations of heat pipe," Mathematical and Computer Modelling, vol. 57, no. 1–2, pp. 126–136, Jan.

2013, doi: https://doi.org/10.1016/j.mcm.2011.06.047.

[11] M. Hammad, "Experimental study of the performance of a solar collector cooled by heat pipes," Energy Conversion and Management, vol. 36, no. 3, pp. 197–203, Mar. 1995, doi: https://doi.org/10.1016/0196-8904(94)00050-a.

[12] H. Ma et al., "Experimental study on heat pipe assisted heat exchanger used for industrial waste heat recovery," Applied Energy, vol. 169, pp. 177–186, May 2016, doi: https://doi.org/10.1016/j.apenergy.2016.02.012.

[13] Kyung Mo Kim, Yeong Shin Jeong, In Guk Kim, and In Cheol Bang, "Comparison of thermal performances of water-filled, SiC nanofluid-filled and SiC nanoparticles-coated heat pipes," International Journal of Heat and Mass Transfer, vol. 88, pp. 862–871, Sep. 2015, doi: https://doi.org/10.1016/j.ijheatmasstransfer.2015.04.108.

[14] Y.-C. Weng, H.-P. Cho, C.-C. Chang, and S.-L. Chen, "Heat pipe with PCM for electronic cooling," Applied Energy, vol. 88, no. 5, pp. 1825–1833, May 2011, doi: https://doi.org/10.1016/j.apenergy.2010.12.004.

[15] C. Shi, Y. Wang, Q. Liao, and Y. Yang, "Analysis and application of variable conductance heat pipe air preheater," Journal of Thermal Science/Journal of thermal science, vol. 20, no. 3, pp. 248–253, May 2011, doi: https://doi.org/10.1007/s11630-011-0466-5.

[16] M. Hu, R. Zheng, G. Pei, Y. Wang, J. Li, and J. Ji, "Experimental study of the effect of inclination angle on the thermal performance of heat pipe photovoltaic/thermal (PV/T) systems with wickless heat pipe and wire-meshed heat pipe," Applied Thermal Engineering, vol. 106, pp. 651–660, Aug. 2016, doi: https://doi.org/10.1016/j.applthermaleng.2016.06.003.

[17] J. Seo and J.-Y. Lee, "Length effect on entrainment limitation of vertical wickless heat pipe," International Journal of Heat and Mass Transfer, vol. 101, pp. 373–378, Oct. 2016, doi: https://doi.org/10.1016/j.ijheatmasstransfer.2016.05.096.

[18] S. Hong, X. Zhang, S. Wang, and Z. Zhang, "Experiment study on heat transfer capability of an innovative gravity assisted ultra-thin looped heat pipe," International Journal of Thermal Sciences, vol. 95, pp. 106–114, Sep. 2015, doi: https://doi.org/10.1016/j.ijthermalsci.2015.04.003.

[19] D. Li, Z. Huang, X. Liao, S. Zu, and Q. Jian, "Heat and mass transfer characteristics of ultra-thin flat heat pipe with different liquid filling rates," vol. 199, pp. 117588–117588, Nov. 2021, doi: https://doi.org/10.1016/j.applthermaleng.2021.117588.

[20] Yu.E. Nikolaenko et al., "Experimental study on characteristics of gravity heat pipe with threaded evaporator," Thermal science and engineering progress, vol. 26, pp. 101107–101107, Dec. 2021, doi: https://doi.org/10.1016/j.tsep.2021.101107.

[21] X. Chen, H. Ye, X. Fan, T. Ren, and G. Zhang, "A review of small heat pipes for electronics," Applied Thermal Engineering, vol. 96, pp. 1–17, Mar. 2016, doi: https://doi.org/10.1016/j.applthermaleng.2015.11.048.

[22] B. Orr, A. Akbarzadeh, M. Mochizuki, and R. Singh, "A review of car waste heat recovery systems utilising thermoelectric generators and heat pipes," Applied Thermal Engineering, vol. 101, pp. 490–495, May 2016, doi: https://doi.org/10.1016/j.applthermaleng.2015.10.081.

[23] L. Ling, Q. Zhang, Y. Yu, and S. Liao, "A state-of-the-art review on the application of heat pipe system in data centers," Applied Thermal Engineering, vol. 199, p. 117618, Nov. 2021, doi: https://doi.org/10.1016/j.applthermaleng.2021.117618.

[24] K. Nakamura, K. Odagiri, and H. Nagano, "Study on a loop heat pipe for a long-distance heat transport under anti-gravity condition," Applied Thermal Engineering, vol. 107, pp. 167–174, Aug. 2016, doi: https://doi.org/10.1016/j.applthermaleng.2016.06.162.

[25] J. Zhang, Y. H. Diao, Y. H. Zhao, X. Tang, W. J. Yu, and S. Wang, "Experimental study on the heat recovery characteristics of a new-type flat micro-heat pipe array heat exchanger using nanofluid," Energy Conversion and Management, vol. 75, pp. 609–616, Nov. 2013, doi: https://doi.org/10.1016/j.enconman.2013.08.003.

[26] D. A. Reay, P. A. Kew, R. J. Mcglen, and P. Firm, Heat pipes: theory, design and applications. Burlington: Elsevier Science, 2013.

[27] S. J. Kline, "The Purposes of Uncertainty Analysis," Journal of Fluids Engineering, vol. 107, no. 2, pp. 153–160, Jun. 1985, doi: https://doi.org/10.1115/1.3242449.

[28] Kyung Mo Kim and In Cheol Bang, "Heat transfer characteristics and operation limit of pressurized hybrid heat pipe for small modular reactors," Applied thermal engineering, vol. 112, pp. 560–571, Feb. 2017, doi: https://doi.org/10.1016/j.applthermaleng.2016.10.077.

[29] V. Guichet, S. Almahmoud, and H. Jouhara, "Nucleate pool boiling heat transfer in wickless heat pipes (two-phase closed thermosyphons): A critical review of correlations," Thermal Science and Engineering Progress, vol. 13, p. 100384, Oct. 2019, doi: https://doi.org/10.1016/j.tsep.2019.100384.

Appendix 1: Uncertainty Analysis

In the present study, the uncertainty in various performance parameters was estimated in accordance with the procedure given by Kline and McClintock. The details of uncertainty in the measurement of different parameters by various instruments are given in Table 2.

Table 2: Uncertainty of various instruments.

Variable	Instrument	Uncertainty (ω)
Temperature (T)	RTD Sensor	0.1°C
Voltage (V)	Digital Voltmeter	1 V
Current (I)	Digital Ammeter	0.1 A
Time (t)	Stopwatch	0.1 s
Length of water column (l)	Measuring Cylinder	2 ml
Length of pipe (L)	Measuring Tape	1 mm
Diameter of pipe (d)	Vernier Caliper	0.1 mm

The following method was used to evaluate the uncertainty in variable 'y'

$$y = f(x_1, x_2, x_3 \dots x_n) \tag{12}$$

The absolute uncertainty in 'y' is given by

$$\omega_{y,a} = \left[\left(\frac{\partial y}{\partial x_1}\omega_{x_1}\right)^2 + \left(\frac{\partial y}{\partial x_2}\omega_{x_2}\right)^2 + \left(\frac{\partial y}{\partial x_3}\omega_{x_3}\right)^2 + \cdots + \left(\frac{\partial y}{\partial x_n}\omega_{x_n}\right)^2\right]^{1/2} \tag{13}$$

The relative uncertainty in 'y' was estimated as under:

$$\omega_{y,r} = \frac{\omega_{y,a}}{y} \times 100 \tag{14}$$

where, ω_{x_1}, ω_{x_2}, ω_{x_3} are uncertainty in measurements of parameter x_1, x_2 and x_3 respectively.

The relative uncertainty analysis of above parameters was carried out for maximum efficiency. The magnitudes of relative uncertainty for various parameters were found as under:

Overall thermal resistance $\omega_{R_o,r}$ = 2.60%

Overall heat transfer coefficient $\omega_{h_o,r}$ = 1.33%

Heat supplied to the evaporator section $\omega_{Q_e,r}$ = 2.58%

Heat gained by cold water $\omega_{Q_c,r}$ = 0.21%

Efficiency of heat pipe $\omega_{\eta,r}$ = 2.59%